Economic Geology
Vol. 93, 1998, pp. 216–223

SCIENTIFIC COMMUNICATIONS

*ON THE SIGNIFICANCE OF AQUEOUS FLUID INCLUSIONS IN GOLD-BEARING QUARTZ VEIN DEPOSITS FROM THE SOUTHEASTERN ABITIBI SUBPROVINCE (QUEBEC, CANADA)**

ANNE-MARIE BOULLIER,[†]

Laboratoire de Géophysique Interne et Tectonophysique, C.N.R.S., B.P. 53X, F-38041 Grenoble Cedex 9, France

KARIMA FIRDAOUS,

C.R.P.G and C.N.R.S., B.P. 20, F-54500 Vandoeuvre-lès-Nancy Cedex, France

AND FRANÇOIS ROBERT**

Geological Survey of Canada, Energy Mines and Ressources, 601 Booth Street, Ottawa, Ontario, Canada K1A 0E8

Abstract

Fluid inclusions have been studied in a quartz-epidote-actinolite vein within a Proterozoic diabase dike crosscutting the Donalda 1 gold-bearing quartz vein, near Noranda, Quebec. Two types of fluid inclusions were recognized. The first type is represented by two-phase aqueous fluid inclusions characterized by low eutectic ($<-45°C$), variable ice-melting (-33 to $-6°C$), and high homogenization to the liquid phase ($T_{h_{L-V(L)}}$ $>200°C$) temperatures. The second type is represented by two- or three-phase (± solid) aqueous fluid inclusions characterized by low eutectic ($<-45°C$), highly variable ice-melting (-52.8 to $-2.4°C$), low homogenization to the liquid phase ($T_{h_{L-V(L)}}$ $<130°C$), and halite dissolution ($<200°C$) temperatures. This second fluid inclusion type is also described with H_2O-CO_2 and CO_2 fluid inclusions in Archean gold-bearing quartz veins of the southeastern Abitibi belt and has a chemical composition (Ca-Na-Cl-bearing with variable salinity) comparable to that of brines and ground waters found in the Superior province. This study demonstrates that these low T_h aqueous fluids showing variable salinity are unrelated to gold deposition, but should rather be correlated with younger brines and ground waters which percolated downward in the continental crust. In these gold-bearing quartz veins, only the high T_h aqueous fluids may be linked to gold-bearing fluids.

Introduction

IT IS now well established that Archean gold-bearing quartz vein deposits formed from CO_2-bearing, low- to moderate-salinity fluids (see, for example, Kerrich and Wyman, 1990; Ho et al., 1992; Groves et al., 1995). This is demonstrated by the abundance of CO_2-rich and H_2O-CO_2 fluid inclusions in the veins. In addition, aqueous fluid inclusions with highly variable salinities have also been reported from a number of gold-bearing quartz vein deposits in the Superior province in the Chibougamau mining camp by Guha et al. (1979), at Sigma by Robert and Kelly (1987) and Firdaous (1995), at Lamaque by Burrows (1990), and at Hollinger-McIntyre by Smith et al. (1984). Controversy exists as to the significance of such fluid inclusions and their link with gold mineralization. They have been regarded either as the product of unmixing from a parental H_2O-CO_2 fluid of low salinity (Robert and Kelly, 1987) or as representing late basement brines that have percolated through existing veins (Burrows, 1990; Kerrich and King, 1993). Indeed, multiple post-Archean episodes of fracturing and fluid infiltration have been documented in the Superior province by Kamineni et al. (1990) and Kerrich and Kamineni (1988). The purpose of this note is to present new fluid inclusion data that may shed some light on this important problem.

Our approach to this problem has been to examine fluid inclusions in a quartz vein within a Proterozoic diabase dike crosscutting an Archean gold-bearing quartz vein at the Donalda deposit in the Noranda district, southeastern Abitibi belt. This Proterozoic quartz vein provides a sample of the postore fluids that may have overprinted gold-bearing quartz vein deposits. Fluid inclusion data from this vein are then compared with new and existing data from the Sigma and Dumont gold quartz vein deposits in the Val d'Or district.

Description of the Deposits

The gold-bearing quartz deposits of the southeastern Abitibi belt are interpreted to have formed during the late stages of regional north-south D_2 shortening (Robert, 1990; Robert and Poulsen, 1997). They typically consist of laminated fault veins, hosted in high-angle reverse shear zones, and of variably developed subhorizontal extensional veins; both vein types are contemporaneous (Robert, 1990).

Donalda deposit

The geology of the Donalda deposit, located near Rouyn-Noranda, has been described by Riverin et al. (1990) and

Corresponding author: email, ann-marie.boullier@obs.ujf-grenoble.fr
* Contribution Centre de Recherches Pétrographiques et Géochimiques no. 1307, CNRS-INSU "Fluides et Failles" no. 92.
** Present address: Barrick Gold Corporation, 7257 Dunver Crescent, Verdun, Quebec, Canada H4H 2H6.

0361-0128/98/1967/216-8$6.00

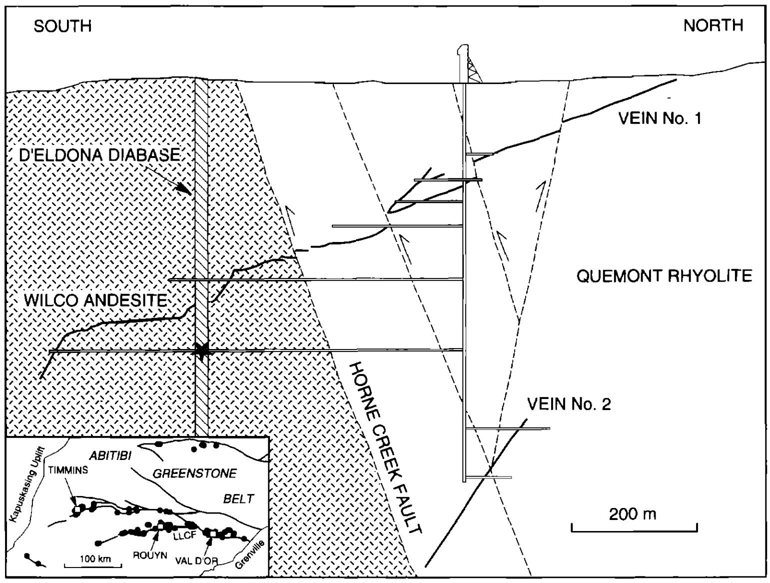

FIG. 1. Schematic cross section of the Donalda mine, after Riverin et al. (1990), showing location of the small late quartz vein crosscutting the d'Eldona diabase dike (black star). Insert: simplified map of the Abitibi subprovince showing the distribution of gold-bearing quartz vein deposits in relation to crustal-scale fault zones. LLCF: Larder Lake-Cadillac fault.

Robert et al. (1996). Of the two veins comprising the deposit, vein 1 is the most extensive, covering an area in excess of 0.5 km^2, at an overall dip of 20° to the south (Fig. 1). This vein consists of alternating vein segments of shallow and moderate dips to the south, the moderate-dipping segments forming relays between larger, shallow-dipping segments (Robert et al., 1996). Vein 1 is crosscut by the D'Eldona diabase dike (Fig. 1) which belongs to a set of northeast-trending dikes of Early Proterozoic age (Buchan et al., 1993). The dike is in turn cut by thin quartz-epidote-actinolite veins that are also subhorizontal. One of these veins has been examined in detail for its fluid inclusions to determine the nature of Proterozoic fluids that have percolated through the deposit (see below).

Sigma deposit

The quartz-tourmaline carbonate vein system at Sigma, located at Val d'Or (Fig. 1), occurs in deformed andesites intruded by preore porphyritic diorite stock and feldspar porphyry dikes. The vein system combines two conjugate sets of steeply dipping shear zone-hosted fault veins and a set of subhorizontal extensional veins. Its structure has been described in detail by Robert and Brown (1986a, 1986b).

Dumont deposit

The Dumont deposit, also located near Val d'Or (Fig. 1), consists of a quartz-tourmaline carbonate vein system within the synvolcanic quartz dioritic Bourlamaque pluton. Veins are mainly hosted by steeply south-dipping reverse shear zones whose location is strongly influenced by the presence of small mafic dikes in the quartz diorite (Belkabir et al., 1993).

Fluid Inclusions

The following paragraphs briefly describe the fluid inclusion methodology followed in this study; see Firdaous (1995) and Robert et al. (1995) for more details.

Generally, fluid inclusions show three modes of occurrence: (1) along grain boundaries of plastically deformed quartz crystals; these have not been measured because most have leaked, (2) in isolated three-dimensional clusters which are considered as primary, and (3) in healed microcracks or fluid inclusion planes which are secondary relative to the host crystal but which provide information on the fluids percolating through the crystal after its crystallization. Microthermometric measurements have been performed on doubly polished sections using a USGS-adapted gas-flow stage calibrated with synthetic fluid inclusions supplied by Synflinc.

Thermometric data from H_2O-CO_2 inclusions were interpreted in terms of composition and density of the trapped fluids using MacFlinCor software (Brown and Hagemann, 1995) and the software of Dubessy et al. (1989) when Raman analyses were available (see Firdaous, 1995, for the details).

Experimental results of Vanko et al. (1988) were used to model the composition of the aqueous fluid inclusions in the H_2O-NaCl-$CaCl_2$ system. Because of the small size of the fluid inclusions (around 5 μm), it was not possible to recognize the different melting phases by temperature cycling during microthermometric measurements; this would have enabled the determination of the bulk composition of the fluid in the ternary plot H_2O-NaCl-$CaCl_2$ (Zwart and Touret, 1994). However, because the isotherms are nearly parallel to the NaCl-$CaCl_2$ side of the plot in the ice field, it was possible to use the ice-melting temperature ($T_{m_{ice}}$) in the undersaturated inclusions to deduce the bulk salinity (NaCl + $CaCl_2$ wt %). Using $T_{m_{ice}}$ and the daughter mineral-melting temperature ($T_{m_{dm}}$) in the saturated inclusions enabled the NaCl/(NaCl + $CaCl_2$) ratio to be estimated graphically (Vanko et al., 1988).

The orientations of secondary fluid inclusion planes have been determined on oriented and doubly polished thick sections according to the procedure described by Boullier et al. (1991). Such fluid inclusion planes represent healed mode I (extensional) microcracks developed in the $\sigma 1$-$\sigma 2$ stress plane, and their different orientations within a given vein must reflect different orientations of the local stress field at different times during the geologic history of the veins (Lespinasse and Pêcher, 1986).

The Donalda deposit

The auriferous veins: Fluid inclusions in vein 1 have been studied by Chi et al. (1992) and their results are summarized in Table 1. They have distinguished three compositional types of fluid inclusions: CO_2-rich, H_2O-CO_2, and aqueous fluid inclusions. The H_2O-CO_2- and CO_2-rich fluid inclusions display similar ranges of CO_2 phase transition temperatures. CO_2 melting occurs between −56.9° and −57.7°C, CO_2 homogenization to the liquid between −30.2° and +30.5°C, and clathrate melting between 3.4° and 8.9°C. Total homogenization temperatures vary from 125° to 367°C to the liquid for H_2O-CO_2 inclusions and from 204° to 328°C to the vapor for CO_2-rich inclusions. The aqueous inclusions display eutectic temperatures (T_e) below −50°C and variable salinities depending on the presence or absence of daughter minerals. Homogenization temperatures to the liquid phase ($Th_{L\text{-}V(L)}$) range from 100° to 380°C with apparent concentration of values between 160° and 220°C.

The barren Proterozoic vein: The vein studied is subhorizontal and 2.5 cm thick. The core of the vein is made of large, clear, and undeformed quartz crystals and green actinolite needles; rosettes of yellowish-green prismatic epidote crystals and interstitial calcite and chlorite are attached to both vein walls (Fig. 2). The D'Eldona diabase is hydrothermally altered at the vein walls and shows an albite-actinote-epidote-titanite-chlorite paragenesis and calcite veinlets.

Fluid inclusions within this vein are of two types. Type 1 inclusions are two-phase aqueous inclusions with a low degree of fill (less than 0.85). They occur as isolated inclusions, in clusters (groups of a few fluid inclusions), or more rarely, in healed microfractures which display some stretching textures. Fluid inclusions of this type do not contain daughter crystals. Their microthermometric characteristics are summarized in Table 1. The first melting (T_e) occurs generally at low temperature (Fig. 3A) between −47° and −67.4°C and indicates the presence of cations other than Na^+ in the solution (Crawford, 1981). The ice-melting temperatures ($T_{m_{ice}}$) are also relatively low and variable (between −6° and −32.6°C; Fig. 3B). Where observed, homogenization (T_h) always occurs to the liquid phase at temperatures above 200°C (Fig. 3C). However, many type 1 fluid inclusions do not homogenize before temperatures up to 460°C and some decrepitate before they homogenize.

Type 2 inclusions consist of liquid-rich (degree of fill higher

TABLE 1. Synthesis of Microthermometric Data (°C) on Fluid Inclusions in Samples from the Donalda, Sigma, and Dumont-Bras d'Or Deposits

Deposit	CO_2-rich fluid inclusions	H_2O-CO_2 fluid inclusions	H_2O-NaCl-$CaCl_2$ fluid inclusions type 1	H_2O-NaCl-$CaCl_2$ fluid inclusions type 2
Donalda gold-bearing quartz veins (Chi et al., 1992)	$T_{m_{CO_2}}$ = −57.5 to −57.2 $T_{h_{CO_2 L\text{-}V(L)}}$ = −30.2 to +28.4 $T_{m_{clathrate}}$ = +8.3 T_{h_V} = 204 to 328	$T_{m_{CO_2}}$ = −57.7 to −56.9 $T_{h_{CO_2 L\text{-}V(L)}}$ = −23.3 to +30.5 $T_{m_{clathrete}}$ = +3.4 to +8.9 T_{h_L} = 125 to 367	With or without daughter mineral (dm) T_e < −50 $T_{m_{ice}}$ = −40.3 to −2.4 $T_{h_{L-V(L)}}$ = 100 to 380	
Donalda Proterozoic quartz vein (this study)			Without daughter mineral T_e = −67.4 to −46.4 $T_{m_{ice}}$ = −32.6 to −6 $T_{h_{L-V(L)}}$ = 212 to >450 T_d often lower than T_h	Without (a) or with (b) daughter mineral T_e = −77 to −28.8 $T_{m_{ice}}$ = −52.8 to −2.4 $T_{h_{L-V(L)}}$ = 29.6 to 186.1 115 < $T_{m_{dm}}$ < 186.8
Sigma gold-bearing quartz veins (Firdaous, 1995)	$T_{m_{CO_2}}$ = −63 to −56.7 $T_{h_{CO_2 L\text{-}V(L or V)}}$ = −49.2 to +29.6	$T_{m_{CO_2}}$ = −63.7 to −56.7 $T_{h_{CO_2 L\text{-}V(L)}}$ = −49.2 to +30.9 $T_{m_{ice}}$ = −10.7 to −0.2 $T_{m_{clathrate}}$ = +6.4 to +14.7 $T_{h_{L\ or\ V}}$ = 211.5 to 425 T_d = 202 to 398.2	Without daughter mineral T_e = −72 to −45.9 $T_{m_{ice}}$ = −51.2 to −1 $T_{h_{L-V(L)}}$ = 249.2 to 366.9	Without (a) or with (b) daughter mineral T_e = −78 to −32.8 $T_{m_{ice}}$ = −49.4 to −1 $T_{h_{L-V(L)}}$ = 60.5 to 222 $T_{m_{dm}}$ = 112.9 to 208.6
Dumont-Bras d'Or gold-bearing quartz veins (Firdaous, 1995)	$T_{m_{CO_2}}$ = −56.8 $T_{h_{CO_2 L\text{-}V(L)}}$ = −8.8 to +5	$T_{m_{CO_2}}$ = −58.2 to −56.6 $T_{h_{CO_2 L\text{-}V(L)}}$ = −0.4 to +30 $T_{m_{ice}}$ = −23.6 to −13.9 $T_{m_{clathrate}}$ = −3.8 to +4.5 T_{h_L} = 211.4 to 376.8 T_d = 238 to 397.6		Without (a) or with (b) daughter mineral T_e = −71.5 to −52.2 $T_{m_{ice}}$ = −42.2 to −16.2 $T_{h_{L-V(L)}}$ = 61.8 to 204 $T_{m_{dm}}$ = 175 to 194

Abbreviations: $T_{m_{CO_2}}$ = melting temperature of the carbonic phase; $T_{h_{CO_2 L\text{-}V(L or V)}}$ = homogenization temperature of the carbonic phase to the liquid (L) or to the vapor(V); $T_{m_{clathrate}}$ = melting temperature of the clathrate; $T_{h_{L\ or\ V}}$ = total homogenization to the liquid (L) or to the vapor phase (V); T_d = decrepitation temperature; T_e = temperature of the eutectic; $T_{m_{ice}}$ = melting temperature of ice; $T_{m_{dm}}$ = melting temperature of the daughter mineral; $T_{h_{L-V(L\ or\ V)}}$ = total homogenization to the liquid (L) or to the vapor (V) phase

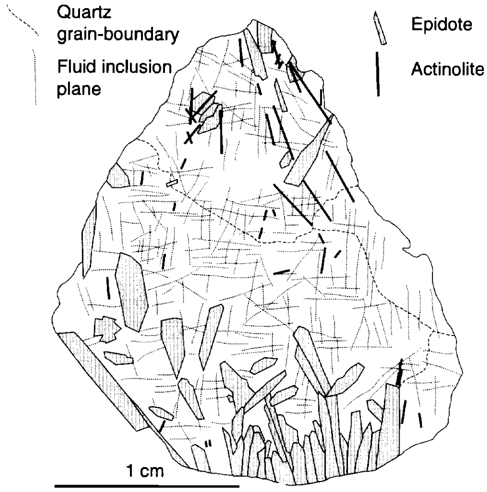

FIG. 2. Line drawing of the doubly polished thick section used for fluid inclusion study from the small Proterozoic quartz vein at Donalda. Sample 92RAO124.

than 0.90), two-phase aqueous inclusions without (type 2a) or with (type 2b) one or more daughter minerals (cube, needle, platelet). They always occur along healed microfractures (or fluid inclusion planes) which show variable degrees of stretching out of the microfracture plane. Based on observed crosscutting relationships, type 2 fluid inclusions are interpreted to be younger than type 1 fluid inclusions. Eutectic temperatures are similar to those of type 1 fluid inclusions but are more scattered (from −28.8° to −77°C, Fig. 3A) and they also indicate the presence of ions other than Na^+ in the solution. SEM-EDA studies show that Ca and Na are the dominant cations recognized in salts precipitated from inclusion decrepitates and have confirmed the presence of halite, sylvite, barite, and calcite daughter minerals (Boullier, unpub. data). Ice-melting temperatures are highly variable (between −2.4° and −52.8°C, Fig. 3B) from one microfracture to another for both type 2a and 2b inclusions but are relatively constant in a single microfracture. Homogenization occurs to the liquid phase at temperatures lower than 130°C (Fig. 3C); some variability (up to 30°) observed in a single microfracture is attributed to stretching. In type 2b inclusions, halite generally disappears at temperature ($T_{m_{dm}}$) higher than bubble disappearance but below 200°C (Fig. 3D). However, since the volume ratio of the salt cube in the inclusion is constant in a single fluid inclusion plane, this feature ($T_{m_{dm}} > T_{h_{L-V(L)}}$) is attributed to the trapping of a homogeneous fluid.

Microthermometric results are consistent with the aqueous nature of both types of fluid inclusion in the vein. This has been confirmed by Raman investigations during which neither CO_2 nor other volatile components could be detected (Firdaous, 1995).

The orientation of only a few planes of type 1 fluid inclusions could be measured and they are nearly parallel to the vein walls (Fig. 4a). Type 2 fluid inclusion planes display similar orientations irrespective of the absence (Fig. 4b) or presence (Fig. 4c) of daughter crystals. These planes are mostly at high angles to the vein walls, but some are also subparallel to the vein walls.

The Sigma deposit

Fluid inclusions of the Sigma deposit have been studied by Robert and Kelly (1987), Firdaous (1995), and Robert et al. (1995). Three main types of fluid inclusions have been recognized in shear-zone-hosted and extensional veins: CO_2-rich inclusions, H_2O-CO_2 inclusions with variable proportions of both phases, and H_2O-rich inclusions with or without solid(s). A fourth type (CH_4-N_2-rich fluid) of inclusions is only sporadically observed. Microthermometric data for CO_2-rich and H_2O-CO_2 inclusions may be summarized as follows (see Table 1): $T_{m_{CO_2}}$ varies between −63.7° and −56.7°C, $T_{h_{CO_2}}$ between −49.2° and 30.9°C, and final homogenization (T_h) of H_2O-CO_2 inclusions ranges from 211° to 425°C, generally to the liquid phase but in a few cases to the vapor phase. The salinity of the aqueous phase of these inclusions is calculated to be between 1 and 6 wt percent NaCl equiv by using $T_{m_{clathrate}}$ (Bozzo et al., 1975; Collins, 1979). The bulk densities of the CO_2-rich and H_2O-CO_2 inclusions calculated with the MacFlinCor software (Brown and Hagemann, 1995) are highly variable.

Two main types of H_2O-rich fluid inclusions have been recognized (Firdaous, 1995): type 1 inclusions have a low degree of fill and are associated with CO_2 and H_2O-CO_2 inclusions in irregular clusters or short microcracks; type 2 have a high degree of fill, are high salinity inclusions without (type 2a) or with (type 2b) a daughter mineral and always occur in late fluid inclusion planes. Both types of H_2O-rich fluid inclusions at Sigma show a wide range of eutectic (between −32.8° and −79°C, Fig. 5A) and ice-melting (between −51.2° and −1°C, Fig. 5B) temperatures. This indicates the presence of ions other than Na^+ in the solution and highly variable salinities. SEM observations have confirmed the presence of halite (Robert and Kelly, 1987) or $CaCl_2$ (Firdaous, 1995) as daughter minerals. Robert and Kelly (1987) also noted that salt hydrates melt at temperatures ranging from −25° to −45°C.

The two types of H_2O-rich fluid inclusions recognized dur-

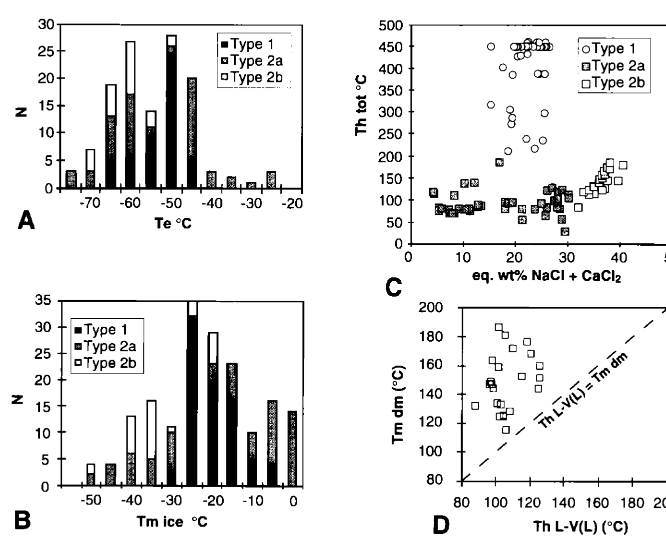

FIG. 3. Microthermometric data for fluid inclusions in the quartz-epidote-actinolite vein crosscutting the Proterozoic diabase at Donalda.

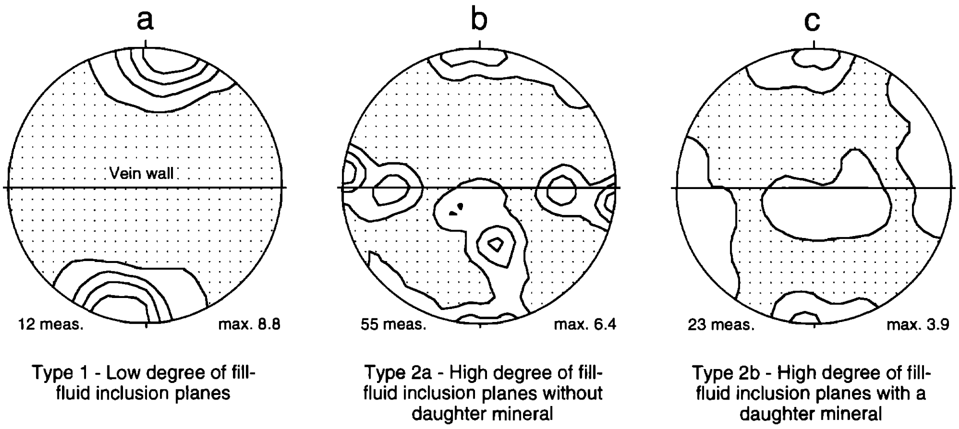

FIG. 4. Stereograms showing the orientation of fluid inclusion planes in sample 92RAO124. Lower hemisphere. Stereoplot software: N. Mancktelow, ETH Zürich. Density contours at 1, 3, 5, and 7 multiples of uniform distribution.

ing petrographic examination are distinguished in the $Th_{h_{total}}$ versus salinity correlation diagram (Fig. 5C). Type 1 fluid inclusions yield high $Th_{h_{total}}$ (>200°C) and high or low salinity values, whereas type 2 inclusions yield low $Th_{h_{total}}$ and display highly variable salinity from one microcrack to the other. They typically homogenize to the liquid phase below 200°C, with some scattering in single microcracks (up to 50°C) probably due to stretching. Inclusions of type 2b homogenize by dissolution of the daughter crystal at $T_{m_{dm}}$ higher than that of vapor bubble disappearance ($Th_{h_{L-V(L)}}$, Fig. 5D) but generally lower than 200°C. However, since the volume ratio of the salt cube in the inclusion is constant in a single fluid inclusion plane, this feature ($T_{m_{dm}} > Th_{h_{L-V(L)}}$) is attributed to the trapping of a homogeneous fluid, as at the Donalda deposit.

Orientations of healed microcracks (fluid inclusion planes) have been measured taking into account the nature of the trapped fluids. Previous results (Boullier and Robert, 1992; Robert et al., 1995; Firdaous, 1995) have shown that a geometric partition of the fluids occurred in extensional veins: CO_2-rich and H_2O-CO_2 fluids are generally trapped in fluid inclusion planes subparallel to the walls of horizontal extensional veins and record vein growth, whereas aqueous fluids mostly occupy subvertical microfractures recording vertical shortening of the veins.

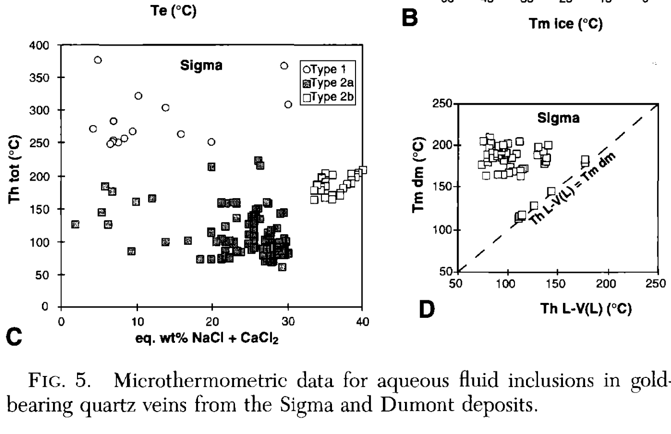

FIG. 5. Microthermometric data for aqueous fluid inclusions in gold-bearing quartz veins from the Sigma and Dumont deposits.

The Dumont deposit

Fluid inclusions of the Dumont deposit have been described by Firdaous (1995) and Robert et al. (1995). The same three main types of fluid inclusions have been recognized as at Sigma (see Table 1). The CO_2-rich and H_2O-CO_2 inclusions display similar microthermometric characteristics at the two deposits, except that at Dumont, $T_{m_{CO_2}}$ is close to that of pure CO_2 (−56.6°C), and the aqueous phase of these inclusions is more saline (10–19 wt % NaCl equiv), as indicated by $T_{m_{clathrate}}$ (−3.8° to +4.5°C range, frequency maximum around +2°C). The bulk density of the CO_2-rich and H_2O-CO_2 inclusions is also highly variable.

Only type 2 (high salinity, high degree of fill) H_2O-rich inclusions have been observed in the samples from the Dumont deposit. They again display the same microthermometric characteristics as those at Sigma: T_e between −52° and −68°C, and $T_{m_{ice}}$ between −16.2° and −41.3°C (Fig. 5A and 5B), indicating $CaCl_2$-rich solutions with variable salinities. Homogenization to the liquid phase occurs between 60° and 200°C.

Interpretation and Implications

A comparison of the fluid inclusion results obtained from the three deposits shows that H_2O-CO_2- and CO_2-rich inclusions are only present in the gold-bearing quartz veins, supporting the conclusions of numerous previous studies that they are related to gold deposition. On the contrary, H_2O-rich fluid inclusions are present both in the gold-bearing quartz veins and in the Proterozoic vein and warrant further consideration.

The microthermometric data for the aqueous fluid inclusions and SEM observations suggest that the system H_2O-

NaCl-$CaCl_2$ (Vanko et al., 1988) can be used, at least as a first approximation, to model their composition and to construct total homogenization versus bulk salinity (wt % NaCl + $CaCl_2$ equiv) diagrams (Figs. 3C and 5C). The NaCl/(NaCl + $CaCl_2$) ratio has been estimated graphically for type 2a saturated inclusions (Vanko et al., 1988). It ranges from 0.3 to 0.4 in the Proterozoic vein at Donalda, and from 0.4 to 0.9 at Sigma (Fig. 6).

Two main groups of aqueous fluids have been observed in the Proterozoic vein at Donalda (Fig. 3C): high $T_{h_{total}}$ (type 1) and low $T_{h_{total}}$ (type 2) fluid inclusions. Because of the simple geologic history of the diabase dike hosting the vein, it is reasonable to attribute the formation of the quartz-epidote-actinolite vein to thermal contraction of the dike during isobaric cooling, and the high $T_{h_{total}}$ fluid inclusions (type 1) to hot fluid infiltration within that vein. These fluids were probably generated by thermally induced ground-water convection around the dike. They may be considered as contemporaneous with vein formation because of their orientation (planes parallel to the vein walls) and their high $T_{h_{total}}$.

The low $T_{h_{total}}$ (types 2a and 2b) fluid inclusions at Donalda are clearly later than type 1 inclusions. They are similar to the low $T_{h_{total}}$ (types 2a and 2b) aqueous fluids encountered in the gold-bearing quartz veins at Sigma and Dumont (Fig. 5C) and to some of the aqueous fluids described by Chi et al. (1992) in the gold-bearing quartz vein at Donalda. They show similar microthermometric characteristics (highly variable $T_{m_{ice}}$ and T_e, low $T_{h_{total}}$ or $T_{m_{dm}}$), and similar vertical orientations in subhorizontal veins. Therefore, these low $T_{h_{total}}$ aqueous fluids in auriferous veins are considered to be equivalent to the fluids observed in the small Proterozoic quartz vein at Donalda and are unrelated to gold deposition.

These low $T_{h_{total}}$ (type 2) aqueous fluid inclusions should be distinguished from the few high $T_{h_{total}}$ (type 1) aqueous fluids that have also been described in the gold-bearing quartz veins at Sigma (Table 1 and Fig. 5C; Firdaous, 1995; Robert et al., 1995). These type 1 aqueous fluid inclusions are texturally associated with H_2O-CO_2 and CO_2 inclusions and generally occur within short vertical cracks issued from reworking of horizontal H_2O-CO_2 fluid inclusion planes (see Boullier and Robert, 1992, fig. 13). Therefore, they are probably linked to the gold-related fluids (Robert et al., 1995) by unmixing of a primary low-salinity H_2O-CO_2 fluid into two immiscible CO_2-rich and H_2O-rich fluids, as suggested by Robert and Kelly (1987). The fact that such type 1 aqueous fluids are not abundant in gold-bearing quartz veins may depend on the volumetric importance of the unmixing process and also on their mechanical separation from the coexisting carbonic phase due to their contrasted wetting properties (Watson and Brennan, 1987), allowing them to escape in the surrounding rocks.

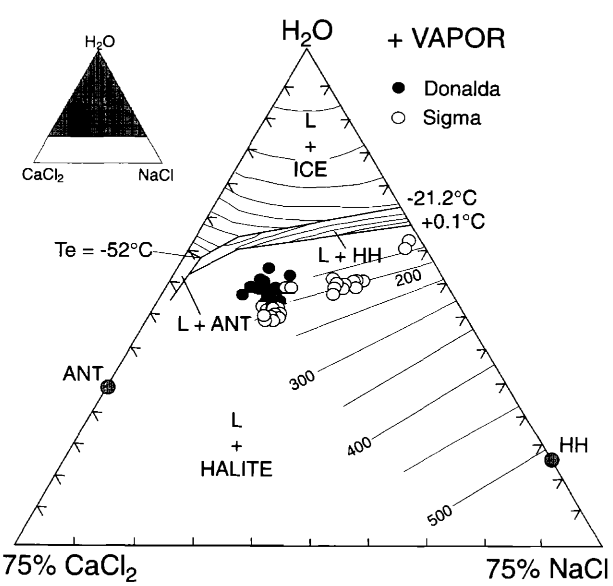

FIG. 6. Phase diagram for NaCl-$CaCl_2$-H_2O (after Vanko et al., 1988) showing the compositions of type 2b aqueous fluid inclusions (with a daughter mineral) in the Donalda late quartz vein and in the Sigma gold-bearing quartz veins. Compositions are in weight percent.

Comparison with Cratonic Brines

Ca-Na-Cl-rich ground waters and brines have been reported from many sites in the Canadian Shield and particularly from many gold mines. Brines may have total dissolved solid concentrations as high as 325 g/l (Frape et al., 1984; Frape and Fritz, 1987; Bottomley et al., 1994). These authors have shown (1) that for a given site, the proportion of the various dissolved species stays relatively constant for variable salinities, (2) that the major anion is chloride and major cations are, first, calcium and, second, sodium, and (3) that the bulk salinity increases with depth.

Three theories have been proposed for the origin of these brines: (1) they represent modified Paleozoic seawater or basinal brines (Kelly et al., 1986; Haynes, 1988; Bottomley et al., 1994); (2) they result from leaching of fluid inclusions (Fritz et al., 1987; Sheppard, 1989); or (3) they result from intense rock-water interactions (Frape and Fritz, 1987; McNutt, 1987) at temperatures as low as 100° to 150°C (Fritz et al., 1994). The brackish and saline ground waters sampled in the Canadian Shield are mixtures of brines and dilute meteoric water according to Frape et al. (1984) and Pearson (1987).

The type 2 aqueous fluids in the late Donalda vein and in the gold-bearing quartz veins from the Sigma and Dumont-Bras d'Or mines are chemically very similar to these Ca-Na-Cl-rich ground waters and brines. Their T_e and SEM analyses of salt precipitates from decrepitated inclusions suggest that Ca is a major cation in the solution. The variable $T_{m_{ice}}$ and $T_{m_{dm}}$ values of these inclusions indicate a highly variable salinity; they show also low and variable $T_{h_{total}}$ values. Therefore, type 2 aqueous fluid inclusions may be interpreted to be the result of mixing in variable proportions of two end-member fluids: a cold fresh ground water percolating downward in the crust in vertical fractures and cracks, and a deep brine which has equilibrated thermally and chemically with the surrounding rocks. Kerrich and Kamineni (1988), on the basis of H, C, and O isotopes and fluid inclusions, have proposed a similar interpretation for adularia- and hematite-bearing veins in the Archean Eye Dashwa pluton in the western Superior province. They also describe liquid-vapor and saturated liquid-vapor fluid inclusions displaying low T_h (140°–230°C) representing $CaCl_2$-NaCl brines. Therefore, infiltration of aqueous and variably saline fluids may represent a widespread or large-scale phenomena.

The maximum daughter mineral-melting temperature measured on the saline aqueous fluid inclusions (ca. 200°C) provides a minimum trapping temperature for these fluids. Assuming a geothermal gradient of 25°C/km for the stable continental crust of the Superior province in the Proterozoic, it is calculated that aqueous fluids have penetrated down to 8 km in the crust. Such a water infiltration may also have induced partial resetting of Archean rocks and vein systems and may account in part for the "young" ages of gold mineralization obtained by the Sm/Nd method on scheelite (Bell et al., 1989; Anglin et al., 1996), the $^{40}Ar/^{39}Ar$ method on vein micas (Hanes et al., 1992; Kerrich and King, 1993), or Rb/Sr whole-rock isochrons (Kerrich, 1986).

Conclusions

The study of fluid inclusions in a quartz-epidote-actinolite vein within a Proterozoic diabase dike at Donalda highlights the existence of two types of aqueous fluids in the history of that vein. First, high homogenization temperatures and variable salinity fluid inclusions are attributed to ground-water convection correlated with the thermal effect of the dike on the surrounding rocks. Fluid inclusions of the second type show low homogenization and eutectic temperatures and highly variable salinities; they represent Ca-Na-Cl fluids which have microthermometric and orientation characteristics similar to those of low T_h, saline aqueous fluids observed in many gold-bearing quartz vein deposits in the Superior province (Boullier and Robert, 1992; Robert et al., 1995; Firdaous, 1995). From this comparison, it is concluded that these latter aqueous fluids are unrelated to the gold deposition. Only rare aqueous fluid inclusions displaying high homogenization temperatures, and spatial and textural association with CO_2- and H_2O-CO_2-rich fluid inclusions in gold-bearing quartz vein deposits may represent the H_2O-rich phase resulting from the unmixing of the primary H_2O-CO_2 low-salinity fluid and may be related in some way to gold deposition.

The Ca-Na-Cl chemistry of the abundant saline and low T_h aqueous fluid inclusions encountered in many gold deposits of many areas within in the Superior province suggests that they are the trapped equivalent of basement brines and ground waters sampled at many sites in the Superior province and that they result from downward percolation of fresh meteoric waters mixing with brines. This phenomenon should be taken into account when interpreting not only fluid inclusion data but also geochronological data because of possible partial resetting of some dated minerals by such fluids.

Acknowledgments

The authors would like to express their appreciation to Gérald Riverin and Bernard Boily, of Inmet Mining Corporation, for their logistic and scientific support. They also gratefully acknowledge Michel Dubois, Véronique Savary, and Simon M.F. Sheppard for fruitfull discussions, as well as Marie-Christine Boiron for Raman analysis. They thank two *Economic Geology* referees for their constructive review of the paper.

June 23, December 12, 1997

REFERENCES

Anglin, C.D., Jonasson, I.R., and Franklin, J.M., 1996, Sm-Nd dating of scheelite and tourmaline: Implications for the genesis of Archean gold deposits, Val d'Or, Canada: ECONOMIC GEOLOGY, v. 91, p. 1372–1382.

Belkabir, A., Robert, F., Vu, L., and Hubert, C., 1993, The influence of dikes on auriferous shear zone development within granitoid intrusions: The Bourlamaque pluton, Val d'Or district, Abitibi greenstone belt: Canadian Journal of Earth Sciences, v. 30, p. 1924–1933.

Bell, K., Anglin, C.D., and Franklin, J.M., 1989, Sm-Nd and Rb-Sr isotope systematics of scheelite: Possible implications for the age and genesis of vein-hosted deposits: Geology, v. 17, p. 500–504.

Bottomley, D.J., Gregoire, D.C., and Raven, K.G., 1994, Saline groundwaters and brines in the Canadian Shield: Geochemical and isotopic evidence for a residual evaporite brine component: Geochimica et Cosmochimica Acta, v. 58, p. 1483–1498.

Boullier, A.M., and Robert, F., 1992, Palaeoseismic events recorded in Archaean gold-bearing quartz vein networks, Val d'Or, Abitibi, Quebec, Canada: Journal of Structural Geology, v. 14, p. 161–179.

Boullier, A.M., France-Lanord, C., Dubessy, J., Adamy, J., and Champenois, M., 1991, Linked fluid and tectonic evolution in the High Himalaya mountains (Nepal): Contributions to Mineralogy and Petrology, v. 107, p. 358–372.

Bozzo, A.T., Chen, H.S., Kass, J.R., and Bardhun, A.J., 1975, The properties of the hydrates of chlorine and carbon dioxide: Desalination, v. 16, p. 303–320.

Brown, P.E., and Hagemann, S.G., 1995, MacFlincor and its application to fluids in Archean lode-gold deposits: Geochimica et Cosmochimica Acta, v. 19, p. 3943–3952.

Buchan, K.L., Mortensen, J.K., and Card, K.D., 1993, Northeast-trending Early Proterozoic dikes of southern Superior province: Multiple episodes of emplacement recognized from integrated paleomagnetism and U-Pb geochronology: Canadian Journal of Earth Sciences, v. 30, p. 1286–1296.

Burrows, D.R., 1990, Relationships between Archaean lode gold quartz vein deposits and igneous intrusions in the Timmins and Val d'Or areas, Abitibi subprovince, Canada: Unpublished Ph.D. thesis, University of Toronto, 226 p.

Chi, G.X., Guha, J., Riverin, G., and Trudel, F., 1992, Examination of an enigmatic flat gold-bearing quartz vein deposit in the Abitibi greenstone belt—a fluid inclusion approach [abs.]: Pan-American Current Research on Fluid Inclusions, 4th biennial conference, Lake Arrowhead, CA, 1992, Abstracts, p. 23.

Collins, P.L.F., 1979, Gas hydrates in CO_2-bearing fluid inclusions and the use of freezing data for estimation of salinity: ECONOMIC GEOLOGY, v. 74, p. 1435–1444.

Crawford, M.L., 1981, Phase equilibria in aqueous fluid inclusions: Mineralogical Association of Canada Short Course Handbook, v. 6, p. 75–100.

Dubessy, J., Poty, B., and Ramboz, C., 1989, Advances in C-O-H-N-S fluid geochemistry based on micro-Raman spectrometric analysis of fluid inclusions: European Journal of Mineralogy, v. 1, p. 517–534.

Firdaous, K., 1995, Etude des fluides dans une zone sismogénique fossile: les Gisements aurifères mésothermaux Archéens de Val d'Or, Abitibi, Québec: Unpublished thèse d'université, Institut National Polytechnique de Lorraine, 332 p.

Frape, S.K., and Fritz, P., 1987, Geochemical trends for groundwaters from the Canadian Shield: Geological Association of Canada Special Paper 33, p. 19–38.

Frape, S.K., Fritz, P., and McNutt, R.H., 1984, Water-rock interaction and chemistry of groundwaters from the Canadian Shield: Geochimica et Cosmochimica Acta, v. 48, p. 1617–1627.

Fritz, B., Clauer, N., and Kam, M., 1987, Strontium isotopic data and geochemical calculations as indicators for the origin of saline waters in crystalline rocks: Geological Association of Canada Special Paper 33, p. 121–126.

Fritz, P., Frape, S.K., Drimmie, R.J., Appleyard, E.C., and Hattori, K., 1994, Sulfate in brines in the crystalline rocks of the Canadian Shield: Geochimica and Cosmochimica Acta, v. 58, p. 57–65.

Groves, D.I., Ridley, J.R., Bloem, E.M.J., Gebre-Mariam, M., Hagemann, S.G., Hronsky, J.M.A., Knight, J.T., McNaughton, N.J., Ojala, J., Vielreicher, R.M., McCuaig, T.C., and Holyland, P.W., 1995, Lode-gold deposits of the Yilgarn block: Products of Late Archean crustal-scale overpressured hydrothermal systems: Geological Society of London Special Publication 95, p. 155–172.

Guha, J., Leroy, J., and Guha, D., 1979, Significance of fluid phases associated with shear zone Cu-Au mineralisation in the Dore Lake Complex, Chibougamou, Quebec: Bulletin de Minéralogie, v. 102, p. 569–576.

Hanes, J.A., Archibald, D.A., Hodgson, C.J., and Robert, F., 1992, Dating of Archean auriferous quartz vein deposits in the Abitibi greenstone belt, Canada: Ar evidence for a 70 to 100 Ma time gap between plutonism-metamorphism and mineralization: ECONOMIC GEOLOGY, v. 87, p. 1849–1861.

Haynes, F.M., 1988, Fluid-inclusion evidence of basinal brines in Archaean basement, Thunder Bay Pb-Zn-Ba district, Ontario, Canada: Canadian Journal of Earth Sciences, v. 25, p. 1884–1894.

Ho, S.E., Groves, D.I., McNaughton, N.J., and Mikucki, E.J., 1992, The source of fluids and solutes in Archaean lode gold deposits of Western Australia: Journal of Volcanology and Geothermal Research, v. 50, p. 173–196.

Kamineni, D.C., Stone, D., and Peterman, Z.E., 1990, Early Proterozoic deformation in the western Superior province, Canadian Shield: Geological Society of America Bulletin, v. 102, p. 1623–1634.

Kelly, W.C., Rye, R.O., and Livnat, A., 1986, Saline mine waters of the Keweenaw Peninsula, northern Michigan: Their nature, origin and relation to similar deep waters in Precambrian crystalline rocks of the Canadian Shield: American Journal of Science, v. 286, p. 281–308.

Kerrich, R., 1986, Fluid transport in lineaments: Royal Society of London Philosophical Transactions, v. A317, p. 219–251.

Kerrich, R., and Kamineni, D.C., 1988, Characteristics and chronology of fracture-fluid infiltration in the Archean, Eye Dashwa Lakes pluton, Superior province: Evidence from H, C, O-isotopes and fluid inclusions: Contributions to Mineralogy and Petrology, v. 99, p. 430–445.

Kerrich, R., and King, R., 1993, Hydrothermal zircon and baddeleyite in Val-d'Or Archean mesothermal gold deposits: Characteristics, compositions, and fluid-inclusion properties, with implications for timing of primary gold mineralization: Canadian Journal of Earth Sciences, v. 30, p. 2334–2351.

Kerrich, R., and Wyman, D., 1990, Geodynamic setting of mesothermal gold deposits: An association with accretionary tectonic regimes: Geology, v. 18, p. 882–885.

Lespinasse, M., and Pêcher, A., 1986, Microfracturing and regional stress field: A study of the preferred orientations of fluid-inclusion planes in a granite from the Massif Central, France: Journal of Structural Geology, v. 8, p. 169–180.

McNutt, R.H., 1987, $^{87}Sr/^{86}Sr$ ratios as indicators of water/rock interactions: application to brines found in Precambrian age rocks from Canada: Geological Association of Canada Special Paper 33, p. 81–88.

Pearson, F.J.J., 1987, Models of mineral controls on the composition of saline groundwaters of the Canadian Shield: Geological Association of Canada Special Paper 33, p. 39–51.

Riverin, G., Bernard, D., and Boily, B., 1990, The Donalda gold deposit, Rouyn-Noranda, Quebec: Canadian Institute of Mining and Metallurgy Special Volume 43, p. 199–209.

Robert, F., 1990, An overview of gold deposits in the eastern Abitibi subprovince: Canadian Institute of Mining and Metallurgy Special Volume 43, p. 93–105.

Robert, F., and Brown, A.C., 1986a, Archean gold-bearing quartz veins at the Sigma mine, Abitibi greenstone belt, Quebec. Part I : Geologic relations and formation of the vein systems: ECONOMIC GEOLOGY, v. 81, p. 578–592.

——1986b, Archean gold-bearing quartz veins at the Sigma mine, Abitibi greenstone belt, Quebec. Part II : Vein paragenesis and hydrothermal alteration: ECONOMIC GEOLOGY, v. 81, p. 593–616.

Robert, F., and Kelly, W.C., 1987, Ore-forming fluids in Archean gold-bearing quartz veins at the Sigma mine, Abitibi greenstone belt, Quebec, Canada: ECONOMIC GEOLOGY, v. 82, p. 1464–1482.

Robert, F., and Poulsen, K.H., 1997, World-class Archaean gold deposits in Canada: An overview: Australian Journal of Earth Sciences, v. 44, p. 329–351.

Robert, F., Boullier, A.M., and Firdaous, K., 1995, Gold-bearing quartz veins in metamorphic terranes and their bearing on the role of fluids in faulting: Journal of Geophysical Research, v. 100, p. 12861–12879.

——1996, Geometric aspects of a large extensional vein, Donalda deposit, Rouyn-Noranda, Quebec: Canada Geological Survey Current Research, v. 1996-c, p. 147–155.

Sheppard, S.M.F., 1989, The isotopic characterization of aqueous and leucogranitic crustal fluids, *in* Bridgwater, D., ed., Fluid movements—element transport and the composition of the deep crust. NATO ASI Series: Dordrecht, Kluwer Academic Press, p. 245–263.

Smith, T.J., Cloke, P.L., and Kesler, S.E., 1984, Geochemistry of fluid inclusions from the McIntyre-Hollinger gold deposit, Timmins, Ontario, Canada: ECONOMIC GEOLOGY, v. 79, 1265–1286.

Vanko, D.A., Bodnar, R.J., and Sterner, S.M., 1988, Synthetic fluid inclusions: VIII. Vapor-saturated halite solubility in part of the system NaCl-$CaCl_2$-H_2O with application to fluid inclusions from oceanic hydrothermal systems: Geochimica et Cosmochimica Acta, v. 52, p. 2451–2456.

Watson, E.B., and Brennan, J.M., 1987, Fluids in the lithosphere. 1: Experimentally determined wetting characteristics of CO_2-H_2O fluids and their implications for fluid transport, host-rock physical properties and fluid inclusion formation: Earth and Planetary Science Letters, v. 85, p. 497–515.

Zwart, E.W., and Touret, J.R.L., 1994, Melting behaviour and composition of aqueous fluid inclusions in fluorite and calcite: Applications within the system H_2O-$CaCl_2$-NaCl: European Journal of Mineralogy, v. 6, p. 773–786.